# Down-regulation of PLCγ2–β-catenin pathway promotes activation and expansion of myeloid-derived suppressor cells in cancer

Aude-Hélène Capietto,[1] Seokho Kim,[1] Dominic E. Sanford,[2] David C. Linehan,[2] Masaki Hikida,[4] Tomohiro Kumosaki,[4] Deborah V. Novack,[3] and Roberta Faccio[1]

[1]Department of Orthopedics, [2]Department of Surgery, [3]Department of Medicine, Washington University School of Medicine, St. Louis, MO
[4]Laboratory for Lymphocyte Differentiation, RIKEN Research Center for Allergy and Immunology, Tsurumi, Yokohama, Kanagawa 230-0045, Japan

**Myeloid-derived suppressor cells (MDSCs) favor tumor promotion, mainly by suppressing antitumor T cell responses in many cancers. Although the mechanism of T cell inhibition is established, the pathways leading to MDSC accumulation in bone marrow and secondary lymphoid organs of tumor-bearing hosts remain unclear. We demonstrate that down-regulation of PLCγ2 signaling in MDSCs is responsible for their aberrant expansion during tumor progression. PLCγ2$^{-/-}$ MDSCs show stronger immune-suppressive activity against CD8$^{+}$ T cells than WT MDSCs and potently promote tumor growth when adoptively transferred into WT mice. Mechanistically, PLCγ2$^{-/-}$ MDSCs display reduced β-catenin levels, and restoration of β-catenin expression decreases their expansion and tumor growth. Consistent with a negative role for β-catenin in MDSCs, its deletion in the myeloid population leads to MDSC accumulation and supports tumor progression, whereas expression of β-catenin constitutively active reduces MDSC numbers and protects from tumor growth. Further emphasizing the clinical relevance of these findings, MDSCs isolated from pancreatic cancer patients show reduced p-PLCγ2 and β-catenin levels compared with healthy controls, similar to tumor-bearing mice. Thus, for the first time, we demonstrate that down-regulation of PLCγ2–β-catenin pathway occurs in mice and humans and leads to MDSC-mediated tumor expansion, raising concerns about the efficacy of systemic β-catenin blockade as anti-cancer therapy.**

CORRESPONDENCE
Roberta Faccio:
faccior@wustl.edu

Abbreviation used: Bax, Bcl-2-associated X protein; β-cat.cKO, β-catenin conditional knockout; β-cat.CA, β-catenin constitutively active; Bcl-2, B-cell lymphoma-2; Bcl-xl, B-cell lymphoma-extra large; BLI, bioluminescence imaging; C/EBP-β, CAAT/enhancer binding protein-β; DAG, diacylglycerol; DCFDA, cellular ROS detection assay; GSK3β, glycogen synthase kinase-3; HPC, hematopoietic progenitor cells; HSC, hematopoietic stem cells; IP3, inositol triphosphate; IRF-8, IFN-regulatory factor 8; ITAM, immunoreceptor tyrosine-based activation motif; ITIM, immunoreceptor tyrosine-based inhibition motif; LLC, Lewis lung carcinoma; LysM, lysozyme M; MDSC, myeloid-derived suppressor cell; M-CSF, macrophage colony-stimulating factor; NO, nitric oxide; PDBu, phorbol 12,13-dibutyrate; PIP2, phosphatidylinositol 4,5-bisphosphate; PIR-B, immunoglobulin-like receptor-B; PKC, protein kinase C; PLCγ2, phospholipase C-γ-2; ROS, reactive oxygen species.

Accumulating evidence indicates that myeloid-derived suppressor cells (MDSCs) are critically involved in tumor progression. Despite the ambiguity surrounding their origin, MDSCs are recognized for their ability to suppress anti-tumor immune responses. MDSCs exert their pro-neoplastic effects through the release of small soluble oxidizers, impairment of T cell/antigen recognition, and depletion of essential amino acids from the local extracellular environment, all ultimately leading to T cell suppression (Mazzoni et al., 2002; Kusmartsev and Gabrilovich, 2003; Liu et al., 2003; Kusmartsev et al., 2004;). Additionally, MDSCs shift immune regulation to a state favoring both tumor escape and proliferation through overproduction of cytokines and angiogenic factors (Kusmartsev and Gabrilovich, 2006). Thus, it is not surprising that presence of MDSCs in the blood and tumor biopsies of cancer patients is associated with poor prognosis (Almand et al., 2001; Lechner et al., 2011; Solito et al., 2011; Porembka et al., 2012).

MDSCs comprise a heterogeneous population of immature myeloid cells (Bronte et al., 2000; Gabrilovich et al., 2001; Liu et al., 2003; Kusmartsev et al., 2004; Kusmartsev et al., 2005; Zea et al., 2005; Gallina et al., 2006), identified by the co-expression of Gr-1 and $\alpha_m$

S. Kim's present address is Korea Research Institute of Bioscience and Biotechnology, 125 Gwahanno, Yuseong-gu, Daejeon 305-806, Korea.



The Rockefeller University Press $30.00
J. Exp. Med. 2013 Vol. 210 No. 11 2257-2271
www.jem.org/cgi/doi/10.1084/jem.20130281

integrin (CD11b) in mice. More recently, MDSCs were subdivided into two different subsets based on the expression of Ly6C and Ly6G. One subset comprises monocytic and mononuclear $CD11b^+Ly6G^-Ly6C^{high}$ cells, called MO-MDSCs, which primarily release NO to suppress T cell activation (Movahedi et al., 2008; Youn et al., 2008). The second subset, termed PMN-MDSCs, includes $CD11b^+Ly6G^+Ly6C^{low}$ cells with granulocytic and polymorphonuclear morphology and they exert T cell inhibition by producing mainly reactive oxygen species (ROS). The expansion of these two MDSC subsets has been shown to be tumor cell line dependent. Most tumors show increased PMN-MDSCs, whereas MO-MDSCs are expanded in only a few models (Youn et al., 2008). Nevertheless, both PMN- and MO-MDSC subsets exert comparable immune suppressive activity primarily against $CD8^+$ T cells.

A large body of work has focused on the identification of the factors modulating MDSC activation and the signals mediating their recruitment to the tumor microenvironment or secondary lymphoid organs. Several tumor-derived growth factors, including macrophage colony-stimulating factor (M-CSF), IL-6, and granulocyte/macrophage colony-stimulating factor (GM-CSF) promote the expansion of MDSCs through stimulation of myelopoiesis and inhibition of the differentiation of mature myeloid cells reviewed by (Gabrilovich and Nagaraj, 2009). Other factors such as IFN-γ, ligands for TLRs, and TGFβ produced mainly by activated T cells and tumor stroma, are involved in MDSC activation. In most instances, phosphorylation of signal transducer and activator of transcription 3 (STAT3) and STAT1 are observed in MDSCs during tumor progression. Although STAT3 was shown to modulate MDSC differentiation and function, recent reports suggest that STAT3 primarily controls the ability of MDSCs to suppress antigen-dependent T cell activation (Kortylewski et al., 2005; Chalmin et al., 2010). Other transcription factors important for myeloid cell fate determination, such as PU.1 (Spi-1) or CAAT/enhancer binding protein-β (C/EBP-β), have been implicated in MDSC differentiation and immunesuppressive functions (Schroeder et al., 2003; Marigo et al., 2010). However, one of the major unresolved questions is the mechanism leading to MDSC expansion in the bone marrow, an event that occurs very early during tumor progression, even when the tumor itself is at a distant site. Thus, the focus of our work is to better understand the mechanisms involved in MDSC accumulation in response to the tumor.

Activation of PLCγ2, an enzyme converting phosphatidylinositol 4,5-bisphosphate (PIP2) into diacylglycerol (DAG) and inositol triphosphate (IP3), is implicated in proliferation and migration of several cancers (Smith et al., 1998; Feng et al., 2012). However, its deletion in the host also leads to increased tumor growth (Zhang et al., 2011). We have recently shown that $PLC\gamma2^{-/-}$ mice are more susceptible to tumor growth in bone despite a decrease in osteoclast number and function. Although PLCγ2 is not required for T cell activation, we observed impaired $CD8^+$ T cell responses in $PLC\gamma2^{-/-}$ tumor-bearing mice (Zhang et al., 2011). Our current study shows that down-regulation of PLCγ2 signaling promotes MDSC expansion in the bone marrow of tumor-bearing mice and enhances MDSC immunosuppressive activities via modulation of β-catenin levels. Together these results highlight a novel molecular pathway regulating the expansion of MDSCs and their crucial role in tumor progression.

## RESULTS

### MDSCs are responsible for increased tumor growth in $PLC\gamma2^{-/-}$ mice

To understand the mechanism responsible for the impaired antitumor T cell response observed in $PLC\gamma2^{-/-}$ mice, we measured the percentage of MDSCs after s.c. inoculation of B16 melanoma and Lewis lung carcinoma (LLC) cell lines. Consistent with a significant increase in s.c. tumor growth in $PLC\gamma2^{-/-}$ mice, we also found a higher percentage of $Gr\text{-}1^+CD11b^+$ MDSCs in the bone marrow, spleen, and tumor site 14 d after inoculation of both tumor cell lines (Fig. 1, A and B). The increase in percentage of MDSCs observed in the null mice was not detected at baseline, reflecting a rather specific response to the tumor itself (not shown). Between the two cell lines, LLC induced stronger MDSC accumulation than B16 cells in both $PLC\gamma2^{-/-}$ and WT mice, and thus this cell line was used for all subsequent experiments. Next, to determine whether the expanded MDSC population observed in the null mice was a consequence of greater tumor growth, we injected WT and $PLC\gamma2^{-/-}$ mice with $10^5$ LLC and sacrificed the animals 7 d after tumor challenge when no detectable differences in tumor weight were yet observed (Fig. 1 C). $PLC\gamma2^{-/-}$ mice already displayed greater MDSC accumulation in bone marrow and spleen, whereas only a small percentage of MDSCs was detected in the tumor at this time in both genotypes (Fig. 1 C).

To determine whether increased numbers of MDSCs are responsible for enhanced tumor growth in $PLC\gamma2^{-/-}$ mice, we adoptively transferred $3 \times 10^6$ MDSCs isolated from LLC tumor-bearing $PLC\gamma2^{-/-}$ or WT mice into WT animals. MDSCs were i.v. injected into the recipient mice 3 and 6 d after s.c. LLC inoculation. Tumor growth was monitored for 2 wk, and the percentage of MDSCs in the spleen was measured at time of sacrifice. We found that adoptive transfer of $PLC\gamma2^{-/-}$ MDSCs into WT recipients significantly enhanced tumor growth compared with animals receiving WT MDSCs, and it also further increased MDSC accumulation in the spleen (Fig. 2 A). To address whether the expansion of MDSCs caused by administration of PLCγ2-deficient MDSCs was caused by proliferation of the null cells or by increased expansion of endogenous MDSCs, we adoptively transferred $CD45.2^+$ $PLC\gamma2^{-/-}$ or WT MDSCs into tumor-bearing $CD45.1^+$ WT recipients. Mice injected with saline were used as controls. Tumor growth was monitored for 14 d and the percentage of endogenous $CD45.1^+$ MDSCs and total $Gr\text{-}1^+CD11b^+$ MDSCs ($CD45.1^+$ and $CD45.2^+$) in the spleen was analyzed at time of sacrifice. As in Fig. 2 A, animals receiving $PLC\gamma2^{-/-}$ MDSCs showed increased tumor growth compared with animals receiving WT MDSCs, accompanied by greater MDSC expansion (Fig. 2 B). Interestingly, the

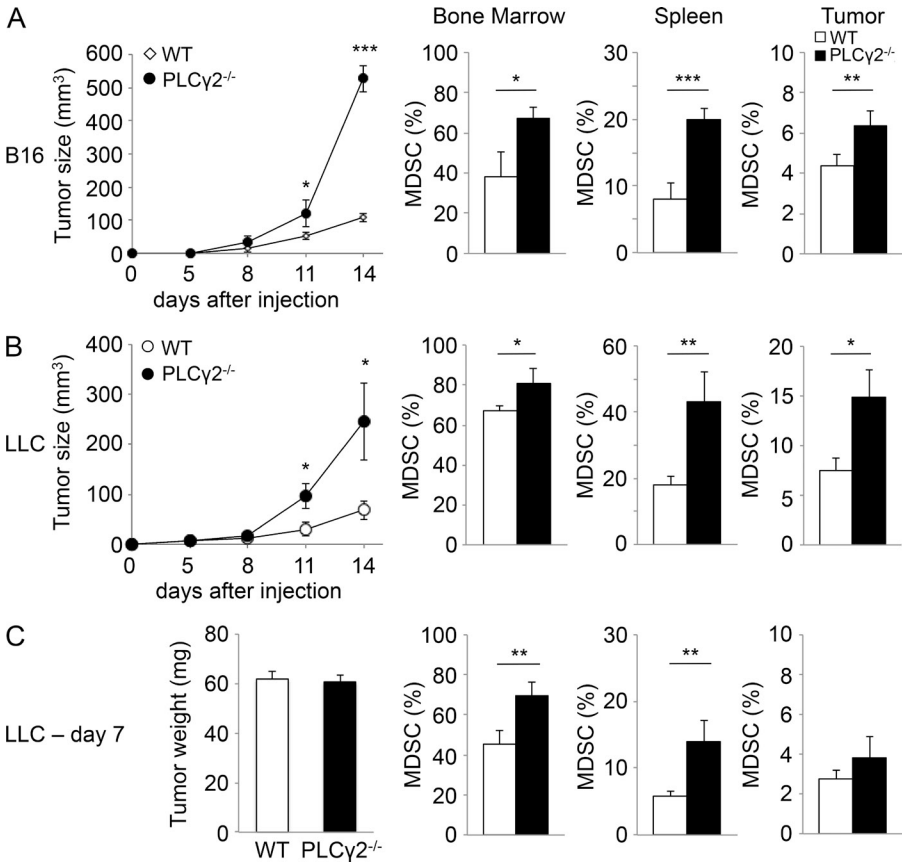


**Figure 1. PLCγ2 deficiency induces greater tumor growth and MDSC accumulation.** (A and B) $10^5$ B16 melanoma (A) or LLC (B) cells were s.c. injected into PLC$\gamma2^{-/-}$ or WT mice and tumor growth was evaluated for 14 d. Percentage of MDSCs in the bone marrow, spleen, and tumor site was analyzed by FACS using anti-Gr-1 and CD11b staining. Results represent mean ± SD (B16: $n = 5$, experiment done in duplicate; LLC: $n = 3$, experiment repeated 4 times). *, $P < 0.05$; **, $P < 0.01$; ***, $P < 0.001$. (C) $10^5$ LLC cells were s.c. injected in PLC$\gamma2^{-/-}$ or WT mice. 7 d after tumor challenge, the tumor was resected and weighed. Percentage of MDSCs from bone marrow, spleen and tumor were then analyzed by FACS staining (Gr-1$^+$CD11b$^+$, MDSCs). Results represent mean ± SD ($n = 4$). Data are reported from one of two similar independent experiments. **, $P < 0.01$.

accumulation of MDSCs after adoptive transfer of either WT or PLC$\gamma2^{-/-}$ cells was due to expansion of endogenous CD45.1$^+$ MDSCs, as their percentage was similar to that of total MDSCs (Fig. 2 B and not depicted). This finding indicates that the transfer of exogenous PLCγ2-deficient MDSCs into WT recipient animals causes the expansion of endogenous MDSCs, which might be the result of enhanced tumor growth. Next, to use a second approach to show that PLCγ2 deficiency in the myeloid population, including MDSCs, is responsible for the observed tumor phenotype, we turned to PLCγ2 conditional KO mice (PLCγ2cKO), in which deletion of PLCγ2 is under control of LysM-Cre. Reduced PLCγ2 expression in MDSCs was confirmed by Western blot, and similarly to the global PLC$\gamma2^{-/-}$ mice, PLCγ2cKO animals also displayed increased tumor growth and MDSC accumulation compared with LysM-Cre controls (not shown).

As MDSCs have also a recognized role in tolerance, we next analyzed whether PLC$\gamma2^{-/-}$ mice, which are on a C57BL/6 background, could allow growth of the allogeneic 4T1 breast cancer cell line derived from BALB/c mice. $5 \times 10^6$ 4T1 tumor cells were inoculated s.c. in WT and PLC$\gamma2^{-/-}$ mice and tumor growth followed for 2 wk. As expected by the different background of the recipient C57BL/6 mice and the 4T1 tumor cell line isolated from BALB/c mice, the tumor engraftment was rejected in WT mice (Fig. 3). However, 4T1 tumor cells grew in PLC$\gamma2^{-/-}$ mice with a concomitant accumulation of MDSCs in the bone marrow and a 2.5 fold-increase in the percentage of MDSCs in the spleen (Fig. 3). All together these results indicate that PLCγ2 is a negative regulator of MDSC expansion and function in tumor-bearing hosts.

### PLCγ2 deficiency favors MDSC accumulation over myeloid cell differentiation in vitro

To better understand the role of PLCγ2 in MDSC accumulation, we isolated MDSCs from the spleen of tumor-bearing mice and analyzed the balance between anti- (Blc-2, Bcl-xl) and proapoptotic (Bax) signals by quantitative RT-PCR. PLC$\gamma2^{-/-}$ MDSCs showed similar relative mRNA expression levels of Bcl-2, Bcl-xl, and Bax to WT MDSCs (not depicted). Next, we wondered whether PLCγ2 deficiency would affect the cell fate differentiation from myeloid progenitor cells in the bone marrow. We isolated lineage negative hematopoietic progenitor cells from PLC$\gamma2^{-/-}$ or WT bone marrow and cultured them in the presence of GM-CSF, IL-4, and tumor conditioned medium (TCM) (Bronte et al., 2000; Youn et al., 2008). After 5 d, we determined the percentage of cells expressing DCs (CD11c), mature DCs (B7.2), macrophages (F4/80), and granulocyte lineage (Gr-1) markers. We found a significant reduction in the percentage of F4/80-positive cells (PLC$\gamma2^{-/-}$: 31.6 ± 1.3% versus WT: 53.3 ± 1.4%; $P = 0.00004$), as well as CD11c (PLC$\gamma2^{-/-}$: 22.3 ± 2.3% versus WT: 35.7 ± 3.0%; $P = 0.004$) and CD11c/B7.2-positive cells (PLC$\gamma2^{-/-}$: 13.8 ± 1.7% versus WT: 24.5 ± 2.2%;

P = 0.003) in the cultures from PLCγ2-deficient cells compared with WT. In contrast, the percentage of Gr-1$^+$ cells was significantly increased in PLCγ2$^{-/-}$ cultures compared with WT (PLCγ2$^{-/-}$: 37.1 ± 0.9% versus WT: 12.0 ± 1.6%; P = 0.0001). This result suggests that PLCγ2 deficiency favors MDSC accumulation over myeloid cell differentiation.

### PLCγ2 deficiency expands PMN- and MO-MDSC subsets and potentiates their immunosuppressive functions

To gain more insights into the role of PLCγ2 in MDSC-induced tumor progression, we performed phenotypic and functional analyses comparing WT and PLCγ2$^{-/-}$ MDSCs during tumor progression. We measured the relative proportion of PMN-MDSCs (CD11b$^+$Ly6G$^+$Ly6C$^{low}$) and MO-MDSCs (CD11b$^+$Ly6G$^-$Ly6C$^{high}$) by FACS in PLCγ2$^{-/-}$ and WT mice. We first confirmed that the percentage of both PMN- and MO-MDSC subsets in bone marrow and spleen was similar at baseline in the two genetic backgrounds (Fig. 4 A). PMN-MDSCs represented the dominant subpopulation before and after the tumor challenge in both WT and KO (Fig. 4, A and B). However, both MDSC subfractions were significantly increased in bone marrow and spleen of PLCγ2$^{-/-}$ mice compared with WT mice in response to LLC-tumor inoculation (Fig. 4 B). Thus, PLCγ2 does not seem to exert differential effects on PMN- and MO-MDSC subsets.

Next, to determine whether PLCγ2$^{-/-}$ MDSCs exhibited stronger immunosuppressive functions compared with WT, in addition to being more numerous, we examined the inhibitory effects of PMN- and MO-MDSCs on T cell proliferation in vitro. As MDSCs were shown to suppress both antigen-driven and mitogen-driven T cell proliferation, we examined the immune-suppressive activity of MDSCs under both conditions. Splenocytes from OT-1 transgenic mice were labeled with CFSE and incubated with MHC class I–restricted SIINFEKL (OT-1) peptide (10 pM) to induce CD8$^+$ T cell antigen–specific proliferation or with anti-CD3 antibody (10 µg/ml) for mitogen-driven CD8$^+$ T cell stimulation. The immune-suppressive effects of MDSCs were determined by culturing WT and PLCγ2$^{-/-}$ PMN- or MO-MDSCs with three different ratios of splenocytes (1:10; 1:5; 1:1). Proliferation of targeted CD8$^+$ T cells was measured in terms of CFSE dilution by flow cytometric analysis 72 h later. We found that both PLCγ2$^{-/-}$ PMN- and MO-MDSCs had greater immune-suppressive effects on CD8$^+$ T cell proliferation than WT MDSCs in both antigen- and mitogen-driven T cell stimulatory conditions (Fig. 5, A and B). It is established that PMN-MDSCs inhibit CD8$^+$ T cell proliferation mainly through ROS production and that MO-MDSCs induce T cell apoptosis mostly via NO release. To evaluate the mechanism by which PLCγ2 deficiency controls MDSC immune suppressive activity, we measured ROS and NO levels in PMN- and MO-MDSCs in response to PMA (300 nM) or LPS (1 µg/ml) for indicated time. As expected (Movahedi et al., 2008; Youn et al., 2008), WT PMN-MDSCs predominantly produced ROS, whereas WT MO-MDSCs mainly released nitrites (Fig. 5, C and D). In contrast, PMN-MDSCs

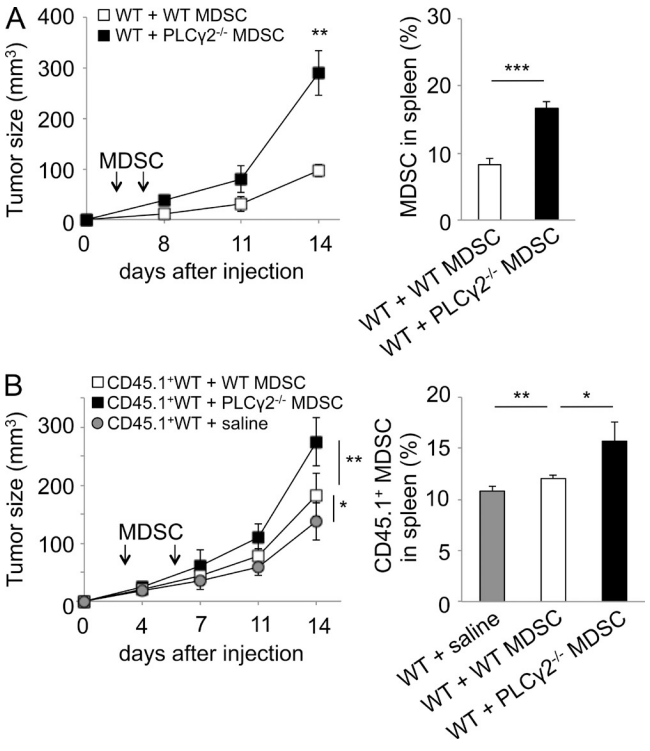


**Figure 2. Adoptive transfer of PLCγ2$^{-/-}$ MDSCs enhances tumor growth in WT mice.** (A) WT mice s.c. inoculated with LLC cells were adoptively transferred on days 3 and 6 with 3 × 10$^6$ WT or PLCγ2$^{-/-}$ MDSCs from LLC tumor–bearing mice. Tumor growth was followed for 14 d, and the percentage of Gr-1$^+$CD11b$^+$ MDSCs isolated from spleens was determined by FACS. Mean ± SD ($n$ = 5) are shown. Data are reported from one of two similar experiments. **, P < 0.01; ***, P < 0.001. (B) 3 × 10$^6$ WT or PLCγ2$^{-/-}$ MDSCs were isolated from the spleen of tumor-bearing CD45.2$^+$ mice and inoculated i.v. into CD45.1$^+$ WT mice on days 3 and 6 after LLC tumor challenge. The tumor growth in CD45.1$^+$ WT recipients was monitored for 14 d, and the percentage of endogenous CD45.1$^+$ Gr-1$^+$CD11b$^+$ MDSCs in spleen was determined by FACS. Mean ± SD ($n$ = 5) are shown. Data are reported from one of two similar independent experiments. *, P < 0.05; **, P < 0.01.


**Figure 3. PLCγ2$^{-/-}$ mice permit 4T1 allogeneic tumor growth.** 5 × 10$^6$ 4T1 mammary tumor cells were s.c. injected in PLCγ2$^{-/-}$ or WT mice and tumor growth was evaluated for 14 d. Percentage of MDSCs in spleen was then analyzed by FACS using anti–Gr-1 and CD11b staining. Results represent mean ± SD ($n$ = 3). One representative experiment of two is shown. *, P < 0.05; **, P < 0.01; ***, P < 0.001.

and MO-MDSCs from PLCγ2$^{-/-}$ mice released both high levels of ROS and NO (Fig. 5, C and D). Thus, PLCγ2 deficiency in both MDSC subsets induces higher release of soluble oxidizers, making them more effective in suppressing both Ag-specific and nonspecific immune responses.

### Reduced β-catenin levels are observed in PLCγ2$^{-/-}$ MDSCs

Dysregulated β-catenin signaling has been noted in many cancers. Furthermore, β-catenin pathway is also known to modulate the self-renewal and maintenance of hematopoietic stem cells and myeloid progenitor cells (Scheller et al., 2006). Because MDSCs are immature myeloid progenitor cells, we hypothesized that β-catenin could be an important player in their development. First, we confirmed deletion of PLCγ2 and reduced phosphorylation levels of the PLCγ2 effector PKC (p-PKC; Fig. 6 A). Next, we measured β-catenin and phosphorylated-GSK3β (p-GSK3β) levels in WT and PLCγ2$^{-/-}$ MDSCs isolated from tumor-bearing mice by Western blot. Surprisingly, we observed a striking decrease in β-catenin and p-GSK3β levels in PLCγ2$^{-/-}$ MDSCs compared with WT (Fig. 6 A). Because PKC has been previously shown to stabilize β-catenin protein levels in T cells (Lovatt and Bijlmakers, 2010), we wondered if reduced PKC activation in PLCγ2$^{-/-}$ MDSCs could be responsible for decreasing β-catenin levels. To address this question, we turned to the DAG-analogue phorbol 12,13-dibutyrate (PDBu), which can induce PKC activation similarly to endogenous DAG but even in the absence of PLCγ2 (Castagna et al., 1982). Whole PLCγ2$^{-/-}$ bone marrow cells were cultured in the presence of PDBu for 18 h, MDSCs were isolated and β-catenin protein levels were determined by Western blot. Results show increased β-catenin protein levels in PLCγ2-deficient MDSCs treated with PDBu compared with untreated cells (Fig. 6 B), indicating that PLCγ2 can regulate β-catenin levels via DAG-dependent PKC activation.

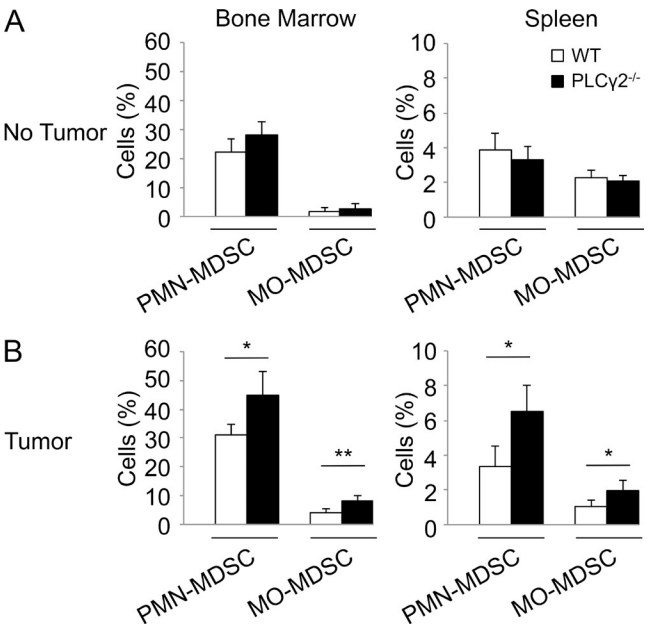


**Figure 4. PLCγ2 deficiency leads to increased PMN- and MO-MDSCs in tumor-bearing mice.** (A and B) Bone marrow and spleens from tumor-free (A, No Tumor) or LLC tumor–bearing (B, Tumor) WT and PLCγ2$^{-/-}$ mice were harvested, and single-cell suspensions were stained for Ly6G and Ly6C markers. Percentages of WT and PLCγ2$^{-/-}$ PMN-MDSCs (CD11b$^{+}$Ly6G$^{+}$Ly6C$^{low}$) and MO-MDSCs (CD11b$^{+}$Ly6G$^{-}$Ly6C$^{high}$) are shown. Data are expressed as mean ± SD ($n$ = 7). Cumulative results from two experiments are shown (A and B). *, P < 0.05; **, P < 0.01.

### β-catenin deficiency in myeloid cells leads to greater tumor growth and MDSC accumulation

To further understand the importance of β-catenin down-regulation in MDSCs in vivo, we turned to the Cre-loxP recombination system to conditionally delete β-catenin in myeloid cells. β-catenin–floxed mice were bred with animals expressing the Cre recombinase under the control of Lysozyme M (LysM-Cre/β-catenin$^{flox/flox}$; herein defined as β-cat.cKO), and deletion of β-catenin in MDSCs was confirmed by Western blot (not shown). We used animals expressing either the Cre recombinase (LysM-Cre/β-catenin$^{wt/wt}$) or the floxed allele (β-catenin$^{flox/flox}$) as a control (CTR). As no differences in tumor growth and MDSC expansion in the two control genotypes were observed, we used either one or the other as control group. LLC tumor cell line was inoculated s.c. into β-cat.cKO or control mice, and tumor growth was followed by caliper measurements for 14 d. The percentage of MDSCs in the bone marrow, spleen, and tumor site was analyzed by flow cytometry at time of sacrifice. Similarly to PLCγ2$^{-/-}$ mice, β-cat.cKO animals displayed greater tumor growth and over twofold increase in the percentage of MDSCs in spleen and tumor site compared with CTR (Fig. 6 C). A significant increase in the percentage of MDSCs in the bone marrow was also observed. To further determine the ability of β-catenin-deficient MDSCs to support tumor growth, we adoptively transferred MDSCs isolated from tumor-bearing β-cat.cKO or CTR mice into tumor-bearing WT mice. Mice receiving saline were used as additional controls. We found that mice transferred with β-cat.cKO MDSCs displayed enhanced tumor volume and twofold increase in splenic MDSCs compared with animals receiving CTR MDSCs or saline (Fig. 6 D).

### β-catenin stabilization in myeloid cells protects from tumor growth by reducing MDSC accumulation and function

To further demonstrate that β-catenin is a critical modulator of MDSC expansion in response to tumor, we turned to a similar LysM-Cre-loxP genetic mouse model to express a constitutively active mutant of β-catenin (LysM-Cre/β-catenin$^{floxEx3/floxEx3}$; herein defined as β-cat.CA; Harada et al., 1999) in myeloid cells, including MDSCs (not shown). LLC cells were inoculated s.c. into β-cat.CA and LysM-Cre CTR mice. Tumor growth was monitored every 2 d, and MDSC accumulation in bone marrow, spleen, and tumor site was evaluated 14 d after tumor challenge. In contrast to β-cat.cKO mice, expression of a stable form of β-catenin in MDSCs reduced tumor growth compared with

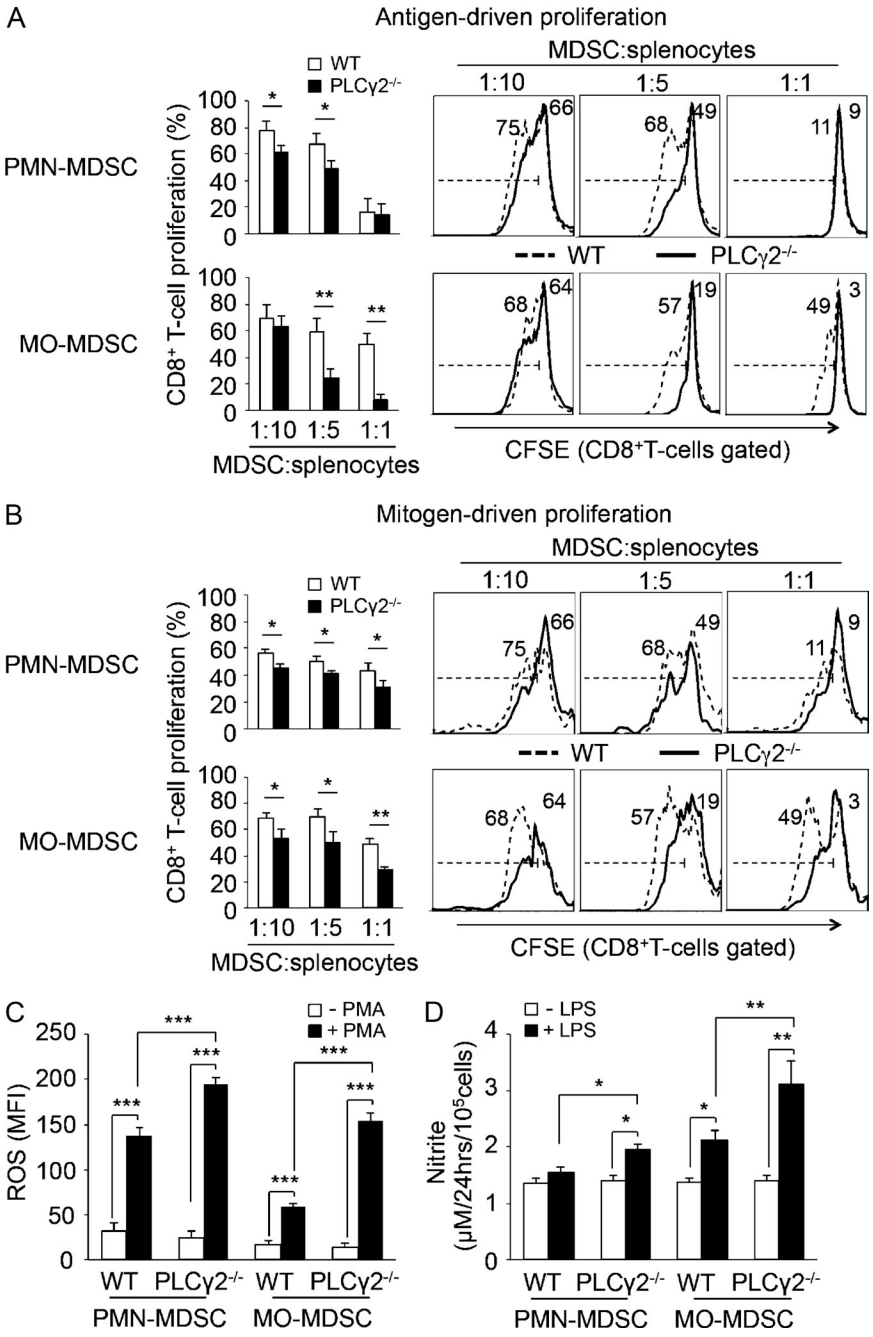


**Figure 5. PLCγ2$^{-/-}$ MDSCs are more potent immune suppressors than WT MDSCs in vitro.** (A and B) T cell proliferation assay. PMN- or MO-MDSCs isolated from WT and PLCγ2$^{-/-}$ mice were co-cultured for 3 d with CFSE-labeled splenocytes from OT-1 transgenic mice (1:10, 1:5, and 1:1 ratios) and stimulated with SIINFEKL peptide (10 pM) in antigen-driven (A) or with anti-CD3 (10 µg/ml) in mitogen-driven (B) experiments. Bar graphs show mean ± SD of three independent experiments. *, P < 0.05; **, P < 0.01. Representative flow cytometric analysis of CD8$^+$ T cell proliferation (shown as CFSE dilution) in the presence of WT (dashed line) and PLCγ2$^{-/-}$ (solid line) MDSCs is also shown. (C and D) Suppressive mechanisms of PMN- and MO-MDSCs isolated from WT and PLCγ2$^{-/-}$ mice. Level of ROS (mean fluorescence intensity, MFI) in PMN and MO subsets in response to PMA stimulation (300 nM for 30 min) was measured using DCFDA staining and FACS. $NO_2$ release in supernatant of $10^5$ MDSCs subfractions was assayed by a standard Greiss reaction after LPS stimulation (1 µg/ml for 24 h; D). Mean ± SD from three independent experiments are shown. *, P < 0.05; **, P < 0.01; ***, P < 0.001.

CTR mice (Fig. 7 A). Although the percentage of MDSCs was not different in the bone marrow, a significant decrease in MDSC accumulation was observed in the spleen and tumor site of β-cat.CA mice (Fig. 7 A). To determine whether stabilization of β-catenin levels in MDSCs would affect their immune suppressive activity in addition to their expansion, we isolated MDSCs from the spleen of tumor-bearing CTR and β-cat.CA mice and co-cultured these cells with WT CFSE-labeled splenocytes at 1:5 and 1:1 ratios. CD8$^+$ T cell proliferation was induced by incubation with anti-CD3 antibody for 72 h and analyzed by FACS. Whereas the T cell proliferation rate was similar in CTR- and β-cat.CA-MDSC cultures at 1:5 ratio, we found that WT MDSCs were more potent inhibitors than β-cat.CA MDSCs at 1:1 ratio (Fig. 7 B). Collectively, these results indicate that modulation of β-catenin levels in MDSCs is critical for their accumulation and function and for modulation of tumor progression.

### β-catenin stabilization in PLCγ2$^{-/-}$ MDSCs decreases their accumulation and immune suppressive activity

Next, to determine if PLCγ2 controls MDSC expansion in response to tumor via β-catenin, we bred LysM-Cre PLCγ2 conditional KO mice (PLCγ2cKO) with LysM-Cre/β-catenin$^{floxEx3/floxEx3}$ mice (β-cat.CA) to obtain the double-mutant PLCγ2cKO/β-cat.CA animals. Because the double

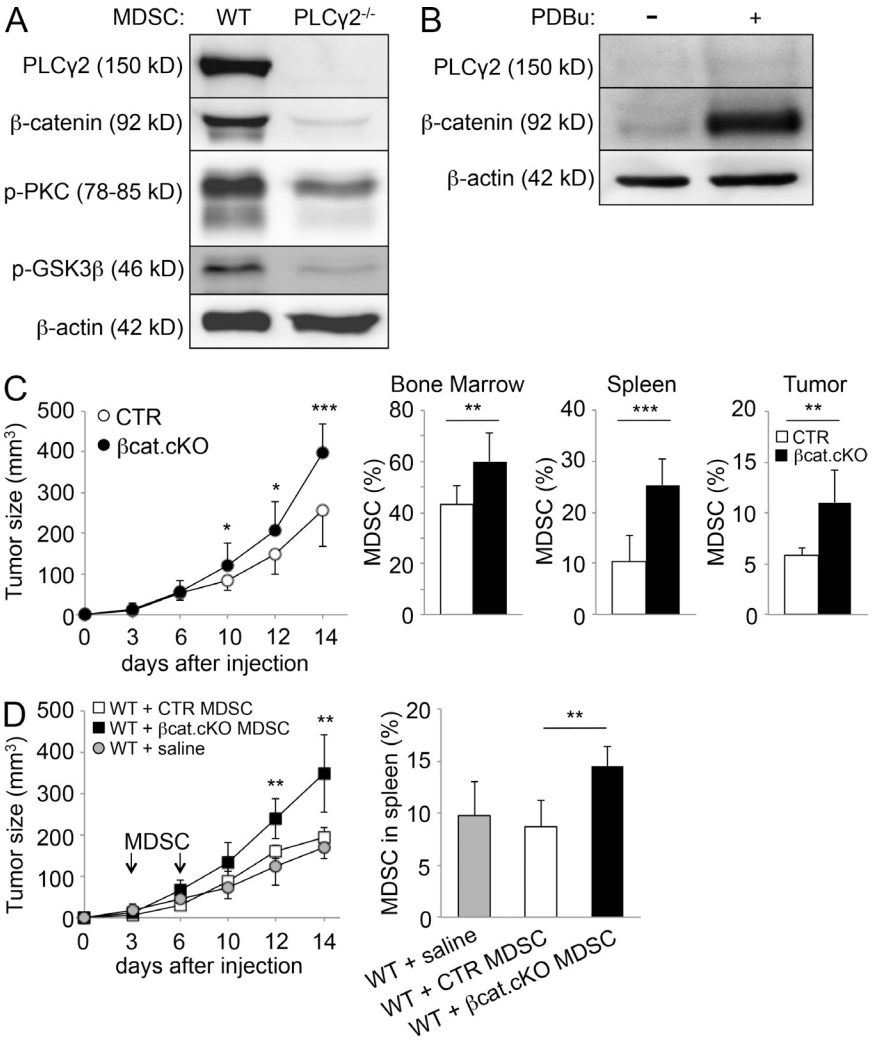


**Figure 6. Down-regulation of β-catenin regulates MDSC accumulation and tumor growth.** (A) Western blot analysis displaying expression levels of PLCγ2, β-catenin, p-PKC and p-GSK3β in MDSCs isolated from tumor-bearing WT and PLCγ2$^{-/-}$ mice. β-actin was used as loading control. One representative blot out of 3 independent experiments is shown. (B) Western blot analysis displaying expression levels of PLCγ2 and β-catenin in PLCγ2$^{-/-}$ MDSCs stimulated with PDBu or saline for 18 h. β-actin was used as loading control. One representative blot out of two independent experiments is shown. (C) $10^5$ LLC cells were s.c. injected in β-cat.cKO or control mice (CTR) and tumor growth followed for 14 d. BM, spleen and tumors were then analyzed by FACS using anti-Gr-1 and CD11b staining to measure the percentage of MDSCs. Mean ± SD ($n$ = 8) are shown. One representative out of 3 independent experiments is shown. *, $P < 0.05$, **, $P < 0.01$, ***, $P < 0.001$. (D) WT mice s.c. inoculated with LLC cells were adoptively transferred on days 3 and 6 with $3 \times 10^6$ CTR- or β-cat.cKO-MDSCs isolated from LLC tumor–bearing mice. Saline injection was used as control. Tumor growth was followed for 14 d. The percentage of MDSCs was determined by FACS in spleen 14 d after tumor inoculation. Mean ± SD ($n$ = 6) are shown. Data are reported from one of two similar independent experiments. **, $P < 0.01$.

mutant mice were born at less than Mendelian rates, rendering the analysis of their tumor phenotype very difficult, we generated radiation chimeras consisting of lethally irradiated WT recipient mice transplanted with bone marrow cells from double-mutant PLCγ2cKO/β-cat.CA animals, PLCγ2cKO or LysM-Cre control mice. 4 wk after bone marrow transplantation, LLC cells were s.c. inoculated into the transplanted mice. Tumor growth was followed for 14 d and the percentage of MDSCs was evaluated by flow cytometry at time of sacrifice. Expression levels of PLCγ2 and β-catenin in MDSCs in all chimeric mice were determined by Western blot (Fig. 7 C). Similar to the global PLCγ2$^{-/-}$ mice, PLCγ2cKO chimeric mice also displayed increased tumor growth and MDSC accumulation compared with LysM-Cre chimeric controls (CTR; Fig. 7 C). In contrast, chimeric mice bearing double-mutant PLCγ2cKO/β-cat.CA bone marrow cells showed significantly lower tumor growth and MDSC expansion than chimeric mice transplanted with PLCγ2cKO cells (Fig. 7 C). To finally determine whether reduced percentage of PLCγ2cKO/β-cat.CA MDSCs was a consequence of decreased tumor growth, we injected CTR, PLCγ2cKO, and PLCγ2cKO/β-cat.CA mice with $10^5$ LLC and sacrificed the animals 5 d after tumor challenge when no detectable differences in tumor weight were yet observed (Fig. 7 D). Similar to the global PLCγ2-deficient mice, we observed greater accumulation of PLCγ2cKO MDSCs compared with CTR in mice with similar tumor size (Fig. 7 D). In contrast, PLCγ2cKO/β-cat.CA mice showed significantly lower MDSC expansion than PLCγ2cKO mice (Fig. 7 D). Consistent with this observation, the percentage of CD8$^+$ T cells infiltrating the tumor was significantly increased in PLCγ2cKO/β-cat.CA compared with PLCγ2cKO (Fig. 7 E). As these findings suggested that stabilization of β-catenin levels in PLCγ2cKO MDSCs impairs cell immune suppressive activity, we performed functional T cell proliferation assays. CTR-, PLCγ2cKO-, and PLCγ2cKO/β-cat.CA-MDSCs were cultured with CFSE-labeled WT splenocytes stimulated with anti-CD3 antibody (10 μg/ml). After 3 d, the proliferation of targeted CD8$^+$ T cells was analyzed in terms of CFSE dilution by flow cytometry. As expected from our previous result (Fig. 5 B), CD8$^+$ T cell proliferation is strongly diminished by PLCγ2cKO MDSCs compared with control. In contrast, PLCγ2cKO/β-cat.CA MDSCs have significantly

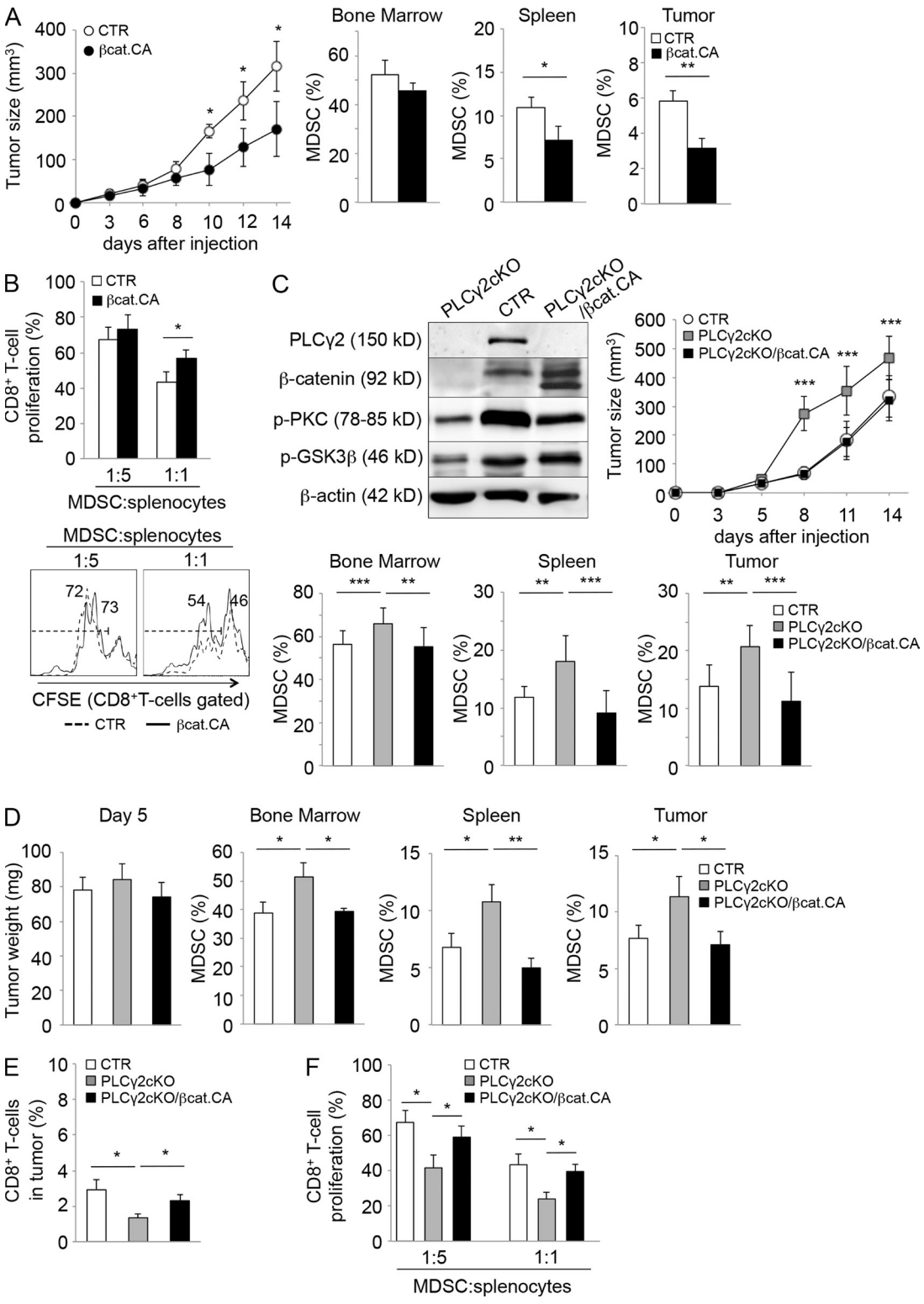


**Figure 7. Increased β-catenin expression inhibits MDSC expansion, activity, and tumor growth.** (A) $10^5$ LLC cells were s.c. injected in β-cat.CA or control mice (CTR), and tumor growth was followed for 14 d. Bone marrow, spleen, and tumors were then analyzed by FACS using anti–Gr-1 and CD11b staining to measure the percentage of MDSCs. Mean ± SD ($n = 4$) are shown. One representative out of two independent experiments is shown. *, $P < 0.05$; **, $P < 0.01$. (B) T cell proliferation assay. MDSCs were isolated from CTR and β-cat.CA mice, co-cultured with CFSE-labeled splenocytes from WT mice (1:5 and 1:1 ratios) and stimulated with anti-CD3 (10 µg/ml) for 3 d. Bar graphs show mean ± SD of three independent experiments. *, $P < 0.05$. Representative flow cytometric analysis of gated CD8⁺ T cell proliferation in the presence of CTR- (dashed line) and β.cat.CA-MDSCs (solid line) is also

less ability to suppress T cell proliferation compared with PLCγ2cKO MDSCs (Fig. 7 F). All together these findings reveal that stabilization of β-catenin in PLCγ2$^{-/-}$ MDSCs modulates MDSC expansion and their suppressive activity.

### Reduced PLCγ2/β-catenin in MDSCs occurs during tumor progression in mice and cancer patients

We then wondered if down-regulation of PLCγ2–β-catenin pathway is an important regulatory mechanism involved in the aberrant MDSC expansion and/or activity during tumor progression. To test the hypothesis that down-regulation of PLCγ2–β-catenin pathway occurs in WT MDSCs, we compared protein expression levels of phosphorylated-PLCγ2 (p-PLCγ2) and β-catenin in MDSCs isolated from tumor-free and tumor-bearing WT mice. Strikingly, we found down-regulation of p-PLCγ2 and β-catenin levels in MDSCs isolated from WT tumor-bearing mice compared with tumor-free controls. Both LLC and B16 tumor cell lines induced a similar phenomenon (Fig. 8 A).

Because various studies implicated MDSCs in the metastatic process (Li et al., 2013; Sawant et al., 2013; Yu et al., 2013), we wondered whether down-regulation of PLCγ2/β-catenin signaling in MDSCs would also occur at late stages of tumor dissemination. To answer this question, we injected firefly-conjugated B16 melanoma (B16-Fl) cells into the left ventricle of WT animals, a model widely used to study tumor dissemination to bone, visceral organs, and lungs in C57BL/6 mice (Arguello et al., 1988; Kang et al., 2003). Animals receiving saline were used as negative control. Recruitment of tumor cells to bone was assessed by bioluminescence imaging. Mice were sacrificed on day 14 when tumor cells were readily detectable in bones, and increased percentage of MDSCs in the bone marrow and the spleen compared with tumor-free controls was confirmed by FACS. Importantly, we also observed reduced p-PLCγ2 and β-catenin protein levels in MDSCs isolated from spleens of animals bearing bone metastases compared with controls (Fig. 8 B). Thus, the down-regulation of PLCγ2–β-catenin axis in MDSCs occurs in mice with primary s.c. tumors as well as during tumor dissemination.

As increased percentage of MDSCs in peripheral blood correlates with disease progression and stage in many human cancers, including pancreatic cancer (Porembka et al., 2012), we isolated MDSCs from PBMCs of pancreatic cancer patients and healthy donors to compare p-PLCγ2 and β-catenin expression levels. Similarly to mice, we isolated the whole human MDSC population, characterized by the co-expression of CD11b and the common myeloid marker CD33 (Greten et al., 2011; Filipazzi et al., 2012). All samples were collected before surgical or medical therapy. 5 patients (49–74 yr of age), 2 with resectable T2A or T3 stages and 3 with unresectable T3 or T4 stages of pancreatic ductal adenocarcinoma were tested by Western blot. Considering the variability between individuals, we normalized protein levels with total amount of protein loaded visualized by β-actin. We found significant reduction of p-PLCγ2 and its downstream effector p-PKC in MDSCs from pancreatic cancer patients compared with healthy donors. β-catenin and p-GSK3β levels were also decreased (Fig. 8 C). In conclusion these results demonstrate that the down-regulation of PLCγ2–β-catenin signaling is a critical step in MDSC expansion in humans and mice.

## DISCUSSION

The mechanism behind MDSC differentiation and the signals that control their commitment and biological function in tumor-bearing hosts are not well understood. MDSCs have been detected in bone marrow, secondary lymphoid organs, and tumor site in many murine tumor models and in patients with advanced malignancies (Young et al., 1988; Gabitass et al., 2011; Porembka et al., 2012). The variability in the percentage of MDSCs and their efficiency to suppress antitumor T cell responses depend on the type and stage of tumor (Youn et al., 2008; Dolcetti et al., 2010; Younos et al., 2011). Several studies focused on identifying tumor-derived factors involved in the accumulation of MDSCs (Bronte et al., 2000; Barreda et al., 2004; Serafini et al., 2006; Pan et al., 2008; Roland et al., 2009; Xiang et al., 2009). Fewer studies, however, analyzed the signaling pathways involved in MDSC expansion in the tumor host. We now provide new evidence demonstrating that down-regulation of PLCγ2 and β-catenin signaling promotes MDSC accumulation in the bone marrow and subsequent recruitment to secondary lymphoid organs and tumor site, where they favor tumor escape from immune control. We found that PLCγ2$^{-/-}$ MDSCs, with reduced β-catenin levels, are increased in number and strongly suppress CD8$^+$ T cell activity via production of ROS and NO species. This increase in MDSC number and immune suppressive effects is likely responsible for the greater s.c growth of LLC and B16 tumor cell lines and for the allogeneic tumor progression

shown. (C) WT mice were lethally irradiated and transplanted with bone marrow cells from PLCγ2cKO, LysM-Cre (CTR), or PLCγ2cKO/β-cat.CA to generate chimeric mice. Western blot analyses show the expression of PLCγ2, β-catenin, p-PKC, p-GSK3β, and β-actin in MDSCs from chimeric mice. 4 wk after BM transplantation, chimeric mice were inoculated s.c. with $10^5$ LLC cells and tumor growth was followed for 14 d. Percentage of MDSCs in bone marrow, spleen, and tumor was analyzed by FACS at time of sacrifice. Mean ± SD ($n$ = 10) are shown. Data are reported from one of two similar independent experiments. **, P < 0.01; ***, P < 0.001. (D and E) $10^5$ LLC cells were s.c. injected in PLCγ2cKO, CTR, or PLCγ2cKO/β-cat.CA mice. 5 d after tumor challenge, the tumor was resected and weighed (D). Percentage of MDSCs from bone marrow, spleen, and tumor were then analyzed by FACS staining (Gr-1$^+$CD11b$^+$, MDSCs) (D). Dissected tumors were stained with anti-CD8 antibody and the percentage of CD8$^+$ T cells was determined by FACS (E). Results represent mean ± SD ($n$ = 3). One representative out of two independent experiments is shown (D and E). *, P < 0.05; **, P < 0.01. (F) T cell proliferation assay. 5 d after LLC tumor inoculation, MDSCs were isolated from CTR, PLCγ2cKO, and PLCγ2cKO/β-cat.CA mice, co-cultured for 3 d with CFSE-labeled splenocytes from WT mice (1:5 and 1:1 ratios), and stimulated with anti-CD3 (10 µg/ml). Bar graphs show mean ± SD of three independent experiments. *, P < 0.05.

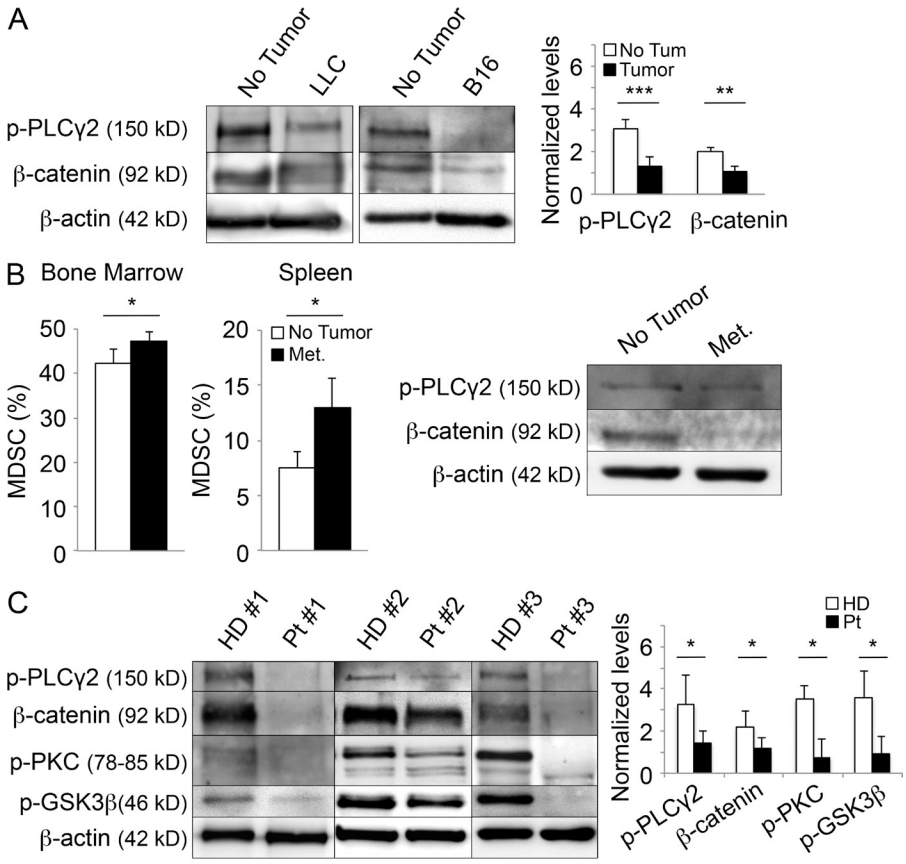


**Figure 8. Reduced p-PLCγ2 and β-catenin expression levels are observed in MDSCs during tumor progression in mice and humans.** (A) Western blot analyses show p-PLCγ2 and β-catenin protein levels in MDSCs from tumor-free (No Tumor) and LLC or B16 tumor-bearing C57BL/6 WT mice. β-actin was used as loading control. Mean ± SD of three tumor-free mice (No Tumor) and three tumor-bearing mice (Tumor). **, $P < 0.01$; ***, $P < 0.001$. (B) $10^4$ B16-Fl cells were i.v. injected in WT mice to allow tumor dissemination to bone. When bone metastases (Met.) were established, animals were sacrificed and bone marrow and spleen were analyzed by FACS using anti–Gr-1 and -CD11b antibodies to measure the percentage of MDSCs. Mice receiving saline i.v. injection were used as controls (No Tumor). Mean ± SD ($n = 4$) is shown. Data are reported from one of two similar independent experiments. *, $P < 0.05$. Western blot analysis of p-PLCγ2, β-catenin and β-actin (loading control) levels in MDSCs from spleen of mice with bone metastases (Met.) or tumor-free controls (No Tumor). One representative Western blot from three different mouse samples is shown. (C) MDSCs isolated from healthy donors (HD) or pancreatic cancer patients (Pt) were analyzed for β-catenin and phosphorylation levels of PLCγ2, PKC, and GSK3β. β-actin was used as loading control. Graph shows semiquantitative analysis of protein levels from Western blots of all samples after normalization to total protein loaded into the gel (measured by β-actin). Three representative patients out of five are shown. *, $P < 0.05$.

of 4T1 breast carcinoma cells observed in PLCγ2$^{-/-}$ mice. Although a tumor/MDSCs vicious cycle is expected to take place, in which larger tumors cause greater MDSC expansion to promote tumor escape from immune control, we found increased PLCγ2$^{-/-}$ MDSCs numbers at early time points after tumor inoculation, when differences in tumor size between WT and KO mice were not present. Although DC and NK cells from PLCγ2$^{-/-}$ mice also have functional defects and could enhance tumor growth in PLCγ2$^{-/-}$ mice, the MDSCs adoptive transfer studies demonstrate that PLCγ2$^{-/-}$ MDSCs alone can greatly increase tumor progression in WT recipient mice. This finding indicates that PLCγ2 controls MDSC development and/or proliferation in response to the tumor.

Enhanced accumulation of MDSCs is also likely to be responsible for the unexpected bone tumor phenotype recently observed in PLCγ2$^{-/-}$ animals (Zhang et al., 2011). In the bone metastasis field, it has been established that bone resorbing osteoclasts are required to sustain tumor growth in bone. Interestingly, PLCγ2$^{-/-}$ mice display enhanced tumor growth in bone despite decreased osteoclast numbers, due to impaired CD8$^+$ T cell activation (Zhang et al., 2011). Thus, expansion of PLCγ2$^{-/-}$ MDSCs in this tumor model seems to overcome the requirement for active osteoclasts to sustain tumor growth in bone. Importantly, the down-regulation of PLCγ2 and β-catenin can also occur in MDSCs from WT mice during tumor dissemination to bone, indicating that PLCγ2/β-catenin pathway modulates MDSC expansion in primary tumors as well as in a metastatic setting.

Similarly to PLCγ2-deficient animals, mice with deletion of β-catenin in the myeloid compartment are more susceptible to tumor growth due to increased MDSC numbers, whereas expression of a constitutively active form of β-catenin decreases MDSC accumulation and tumor growth. Importantly, expression of β-catenin constitutively active in PLCγ2-deficient MDSCs is also sufficient to reduce the expansion and the immune

suppressive activity of PLCγ2$^{-/-}$ MDSCs, allowing greater infiltration of CD8$^+$ T cells at tumor site. Consequently, tumor growth is reduced in PLCγ2cKO/β-cat.CA mice compared with PLCγ2cKO animals. The importance of down-regulation of PLCγ2–β-catenin axis in MDSC accumulation and activity is not limited to our KO mouse models but it is a general mechanism involved in the modulation of WT MDSC responses occurring in the presence of tumor, including in cancer patients. Our data show that pancreatic cancer patients at advanced stage have reduced p-PLCγ2 and β-catenin levels compared with MDSCs isolated from healthy controls. These results demonstrate that PLCγ2 is a negative regulator of MDSC expansion and immune suppressive effects in tumor-bearing hosts via the β-catenin pathway in humans and mice. Several questions arise from this finding.

How is PLCγ2 signaling regulated in MDSCs? Activation of PLCγ2, via phosphorylation of its tyrosine residues, is often observed in hematopoietic cells, including myeloid cells, as well as in cancer cells downstream of ITAM-containing immune receptors, growth factor receptors, and G protein coupled receptors. Considering that the tumor microenvironment is enriched with tumor-derived factors that can potentially signal via PLCγ2, it was very surprising to observe reduction of PLCγ2 phosphorylation in MDSCs from tumor-bearing mice and cancer patients compared with healthy controls. In myeloid cells PLCγ2 activation downstream of ITAM containing receptors can be counterbalanced by negative regulatory signals emanated by receptors containing ITIM domains. A recent study indicated that the ITIM-containing paired immunoglobulin-like receptor (PIR) B is highly expressed in MDSCs (Ma et al., 2011). Deletion of PIR-B switches the MDSC phenotype from immune-suppressive to proinflammatory, thus leading to reduced tumor growth. Therefore, one possible mechanism for down modulation of PLCγ2 activation in WT MDSCs would be through suppression of ITAM signaling by PIR-B. Because β-catenin activation has also been reported to occur downstream of ITAM receptors (Otero et al., 2009), reduced β-catenin levels in MDSCs isolated from tumor-bearing mice or cancer patients could also be caused by suppression of ITAM signaling by PIR-B.

How does PLCγ2 modulate β-catenin? Regardless of which ITAM-containing receptor may activate PLCγ2 and β-catenin, we propose that these molecules lie on the same pathway. This assumption is supported by the observation that β-catenin levels are reduced in PLCγ2$^{-/-}$ MDSCs and that expression of constitutively active β-catenin in PLCγ2$^{-/-}$ marrow cells limits MDSC expansion and immune suppressive effects and reduces tumor growth. Although PLCγ2 has never been shown to directly modulate β-catenin levels, activation of PKC can induce β-catenin stabilization in T cells (Lovatt and Bijlmakers, 2010). It is likely that PKC, a downstream effector of PLCγ2, phosphorylates and thus inactivates GSK3β, a kinase that targets β-catenin for ubiquitination and subsequent proteasomal degradation. In support of this hypothesis, we observed impaired PKC phosphorylation and reduced p-GSK3β levels in PLCγ2$^{-/-}$ MDSCs compared with WT, whereas the rescue of PKC activation by PDBu in PLCγ2$^{-/-}$ MDSCs increases β-catenin protein levels. Nevertheless, we cannot exclude additional PLCγ2-independent down-regulation of β-catenin in MDSCs, possibly via modulation of Wnt ligands or Wnt inhibitors by the tumor cells.

How does β-catenin control MDSC expansion? Elevated levels of β-catenin are often associated with increased cell proliferation. This is especially true for cancer cells. Therefore, it was puzzling to observe that MDSC expansion was associated with reduced β-catenin levels. β-catenin has been extensively analyzed in hematopoiesis, at times leading to contradictory findings. Conditional expression of a stabilized, active form of β-catenin in hematopoietic stem cells (HSC) resulted in hematopoietic failure because of a reduction in cell cycle quiescence, HSC exhaustion, and blocked differentiation. Consistent with our hypothesis that β-catenin limits MDSC expansion, constitutive activation of β-catenin in early hematopoietic precursors significantly reduces the Gr-1$^+$CD11b$^+$ myeloid cell population (Scheller et al., 2006). Thus, it is possible that down-regulation of β-catenin, rather than controlling MDSC proliferation, allows MDSC accumulation by preventing their differentiation into mature myeloid cells. In support of this hypothesis, we find that in vitro cultures of hematopoietic progenitor cells from PLCγ2-deficient mice give rise to less mature myeloid populations but more Gr-1$^+$ cells than WT cultures. Another plausible mechanism that could lead to accumulation of MDSCs in tumor-bearing PLCγ2- and β-catenin–null animals would be through increased differentiation from myeloid progenitors in the bone marrow. Several transcription factors involved in myelopoiesis such as interferon-regulatory factor 8 (IRF-8), C/EBP-β, and PU.1 have been demonstrated to regulate MDSC development (Scheller et al., 1999; Schroeder et al., 2003; Kirstetter et al., 2006; Marigo et al., 2010). However IRF-8, PU.1, and C/EBP-β are also involved in monocyte/macrophage maturation, neutrophil differentiation, and/or DC development (Tamura et al., 2000; Hamdorf et al., 2011; Batliner et al., 2012; Pham et al., 2012). Therefore, further studies are required to determine whether down-regulation of PLCγ2–β-catenin pathway may affect MDSC differentiation via transcriptional regulation.

In conclusion, our results identify the PLCγ2–β-catenin pathway as a negative modulator of MDSC accumulation and activation in response to tumors. This finding is clinically relevant because we confirmed down-regulation of PLCγ2 and β-catenin in human MDSCs isolated from pancreatic cancer patients. This observation is particularly important, as β-catenin targeting is currently in clinical trials because of the positive role of β-catenin on cell growth in many cancers. However, based on our finding this approach could be undermined by tumor escape from immune control through expansion of MDSCs.

## MATERIALS AND METHODS

**Animals and tumor models.** Animals were housed in a pathogen-free animal facility at Washington University. 6–8-wk-old littermate mice were used in all experiments according to protocols approved by the Institutional

Animal Care and Use Committee. PLCγ2$^{-/-}$ mice were on a C57BL/6 background and have been previously described (Wang et al., 2000). WT and PLCγ2$^{-/-}$ littermates were used throughout the study. LysM-Cre/β-catenin$^{flox/flox}$ (conditional KO, β-cat.cKO) and LysM-Cre/β-catenin$^{floxEx3/floxEx3}$ (constitutively active, β-cat.CA) mice on C57BL/6 background were provided by F. Long (Washington University, St. Louis, MO) and have been previously described (Clausen et al., 1999; Harada et al., 1999; Brault et al., 2001). In brief, β-catenin$^{flox/flox}$ mice bear two LoxP sites flanking exons 2–6, which lead to a loss-of-function deletion upon Cre-mediated excision. In β-catenin$^{floxEx3/floxEx3}$ mice, excision of exon 3 leads to a stabilized, non-degradable form of β-catenin. C57BL/6 PLCγ2$^{flox/flox}$ mice were obtained from T. Kurosaki (Kansai Medical University, Moriguchi, Japan; Hashimoto et al., 2000, and the mating strategy to obtain the conditional KO under the LysM-Cre promoter (PLCγ2cKO) was performed in our laboratory. LysM-Cre and floxed littermates were used as controls (CTR). All in vivo figures are shown as representative experiments. Importantly, significant differences are maintained when all CTR groups are pooled together (Fig. 6 C and Fig. 7 A).

CD45.1 C57BL/6 WT mice used for the MDSC transfer experiments were purchased from The Jackson Laboratory. C57BL/6 OT-1 mice were obtained from M. Colonna's laboratory (Washington University, St Louis, MO).

B16 (C57BL/6 murine melanoma cells), LLC (C57BL/6 murine LLC cells), and 4T1 (BALB/c murine mammary tumor cells) were cultured at 37°C in complete media (DMEM supplemented with 2 mM L-glutamine, 100 μg/ml streptomycin, 100 IU/ml penicillin, and 1 mM sodium pyruvate) containing 10% FBS. To establish tumors, B16 ($10^5$), LLC ($10^5$) or BALB/c 4T1 ($5 \times 10^6$) tumor cells were suspended in PBS and inoculated s.c. in the flank of mice. Tumor measurements were performed every 2 or 3 d with a caliper, and volumes were calculated using the following formula: $V = ½ (\text{length [mm]} \times [\text{width \{mm\}}]^2)$.

For adoptive transfer experiments, appropriate control mice and indicated KO (PLCγ2$^{-/-}$ or β-cat.cKO) animals were s.c. injected with $10^5$ LLC. 14 d after tumor xenograft, MDSCs were isolated from the spleen as described below, and $3 \times 10^6$ MDSCs were i.v. injected into WT tumor-bearing mice on days 3 and 6 after tumor challenge. WT mice receiving saline injection on days 3 or 6 were used as additional controls.

$10^4$ firefly-conjugated B16 melanoma cells (B16-Fl) suspended in 50 μl of saline solution were injected into the left cardiac ventricle (i.v.) of 6-wk-old female mice as previously described (Arguello et al., 1988; Kang et al., 2003). Recruitment of tumor cells to bone was monitored on days 9, 12, and 14 by bioluminescence imaging using an IVIS 100 imaging system (Caliper Life Sciences). Mice with extrapleural intrathoracic tumors were excluded from analysis. Bioluminescence photon flux (photons per second) data were analyzed by region of interest measurements in Living Image 3.2 (Caliper Life Sciences).

**Bone marrow transplantation.** 4-wk-old female C57BL/6 mice were lethally irradiated using a 137Cs source with 1,000 rads to generate recipient mice. Bone marrow was harvested from 6-wk-old female PLCγ2cKO, PLCγ2cKO/β-cat.CA, or LysM-Cre control mice. Cells were then suspended in PBS and $10^6$ cells/200 μl were injected into the lateral tail vein of recipient mice. 4 wk after bone marrow transplantation, these mice were inoculated with tumor cells as described above.

**Flow cytometric analysis.** Immediately upon sacrifice, single-cell suspensions were prepared from bone marrow, spleen, and tumor. In brief, bone marrow cells were harvested from tibias and femurs by centrifugation, whereas spleens and tumors were mechanically dissociated and individual cell suspensions obtained through 70-μm cell strainer. Red blood cells were then removed with lysis buffer and cells counted. Cell suspensions were then washed once and stained in PBS with 0.5% FBS with the following anti–mouse antibodies: allophycocyanin (APC)-conjugated anti–Gr-1 or -Ly6C, FITC-conjugated anti-F4/80 (eBioscience); and phycoerythrin (PE)-conjugated antibodies to CD11b or CD11c, FITC-conjugated anti-Ly6G, -CD11c, -CD86 (B7.2), or -CD45.1, APC-conjugated anti-CD8α (BD). The respective isotype-matched conjugated controls were purchased from eBioscience and BD, respectively. Cell surface staining on isolated cells from human PBMCs were performed using monoclonal (PerCP-Cy5.5)-conjugated anti–human CD33 antibody (BioLegend) and (PE)-conjugated anti–human CD11b antibody (BD). Corresponding isotope controls yielded no significant staining. Acquisition was performed on a FACSCalibur and the dedicated software CellQuest (BD). Data were analyzed with FlowJo 7.5.5 software (Tree Star).

**MDSC isolation.** In vivo experiments were assessed using freshly isolated MDSCs from spleens of tumor-bearing mice. Cells were purified by immunomagnetic separation using biotinylated anti–Gr-1 antibody and streptavidin-conjugated MicroBeads with MiniMACS columns according to the manufacturer's protocol (Miltenyi Biotec). In vitro functional and mechanistic assays were done either with whole MDSC population or with PMN- and MO-MDSC subsets. Cells were isolated from spleens of tumor-bearing mice using the Myeloid-Derived Suppressor Cell Isolation kit from Miltenyi Biotec. Cell purity was checked by flow cytometric analysis using anti-CD11b and Gr-1 antibodies (>95%), and viability was checked by Trypan blue dye exclusion.

Human PBMCs were obtained from D.C. Linehan's laboratory (Washington University, St Louis, MO) as previously described (Porembka et al., 2012). In brief, informed consent was prospectively obtained from all patients before obtaining human blood according to the institutionally approved Human Studies Committee Protocol. Peripheral blood samples were collected in vacuum tubes containing EDTA (BD). PBMCs were isolated by Ficoll-density centrifugation and frozen in DMSO with 10% FBS. Cells were then thawed, washed, and processed for cell isolation using CD33 and CD11b MicroBeads with MiniMACS columns according to the manufacturer's protocol (Miltenyi Biotec). Purity was confirmed by flow cytometric (>95%) and Western blot analyses, which were immediately performed.

**Real-time PCR.** MDSCs from spleens were isolated 14 d after tumor challenge as previously described. Total RNA was extracted with TRIzol (Invitrogen) and quantified on ND-1000 spectrophotometer (NanoDrop Technologies). The cDNA was synthesized with 1 μg RNA using RNA to cDNA EcoDry Premix (oligo dT) RT-PCR kit from Takara. The amount of Bcl-2, Bcl-xl, or Bax was determined using *Power* SYBR Green mix on 7300 Real-Time PCR System (Applied Biosystems). Cyclophilin mRNA was used as internal control. Specific primers were as follows: Bcl-2, 5′-TGAGTACCTGAACCGGCATCT-3′ and 5′-GCATCCCAGCCTCCGTTAT-3′; Bcl-xl, 5′-ACAGAGCAGACCCAGTAAGT-3′ and 5′-ACCGCAGTTCAAACTCAT-3′; Bax, 5′-ACAGATCATGAAGACAGGGG-3′ and 5′-CAAAGTAGAAGAGGGCAACC-3′; cyclophilin, 5′-AGCATACAGGTCCTGGCATC-3′ and 5′-TTCACCTTCCAAAAGACCAC-3′. Relative quantification of transcription was calculated as the power of the difference between amplification of the target gene and amplification of cyclophilin (i.e., $2^{-[\text{Ct target gene} - \text{Ct cyclophilin}]}$, where Ct represents threshold cycle).

**Generation of cells from bone marrow progenitors.** Hematopoietic progenitor cells (HPCs) were isolated from WT and PLCγ2$^{-/-}$ bone marrow using the Lineage Cell Depletion kit (Miltenyi Biotec). $5 \times 10^5$ HPCs were cultured in 24-well plates containing 2 ml of RPMI 1640 supplemented with 10% FBS, 20 ng/ml GM-CSF, 10 ng/ml IL-4, and 20% vol/vol tumor conditioned medium (TCM; Youn et al., 2008). The TCM was generated from primary EL-4 tumor cells injected into WT C57BL/6 for 2 wk, collected as single-cell suspension with collagenase and cultured for 2 d in RPMI supplemented with 10% FBS. TCM were frozen at −80°C until further use. After 5 d of HPC cultures, percentages of CD11c$^+$, CD11c$^+$/B7.2$^+$, F4/80$^+$, and Gr-1$^+$ cells in total WT and PLCγ2$^{-/-}$ cell cultures were analyzed by flow cytometry.

**T cell suppression assay.** Freshly isolated splenocytes ($5 \times 10^6$ cells/ml) from OT-I TCR transgenic mice were depleted of red cells and labeled with CFSE (1 μM; Molecular Probe, Carlsbad, CA) for 10 min at 37°C and washed with fresh culture media, according to the manufacturer's instructions. OT-1

splenocytes were specifically stimulated with SIINFEKL peptide (10 pM) or nonspecifically stimulated with anti-CD3 antibody (10 µg/ml). Purified whole MDSC population or PMN- and MO-MDSC subsets from spleen were cultured for 3 d in RPMI 1640 (10% FBS) in U-bottom 96-well plates with $2 \times 10^5$ CFSE-labeled splenocytes at different ratio (1:10, 1:5 and 1,1). Experiments were performed in triplicate. To further analyze the $CD8^+$ T cell proliferation, cells were stained for CD8 and analyzed for CFSE dilution using FACSCalibur. The data are expressed as the percentage of proliferation of stimulated $CD8^+$ $CFSE^+$ T cells.

**ROS and NO production.** The oxidation-sensitive dye DCFDA (Invitrogen) was used to measure ROS production by purified PMN- or MO-MDSCs. Cells were incubated at 37°C in RPMI in the presence of DCFDA (3 µM) and stimulated or not with PMA (300 nM; Sigma-Aldrich) for 30 min. Cells were then washed twice with cold PBS and labeled with anti–Gr-1 and CD11b antibodies before flow cytometric analysis.

Nitrite quantification was assayed by a standard Greiss reaction, as previously described (Liu et al., 2003). In brief, purified $10^5$ PMN- or MO-MDSCs were stimulated with LPS (1 µg/ml) for 24 h in RPMI 1640 media supplemented with 10% FBS and 10 ng/ml GM-CSF. Equal volumes of culture supernatant (100 µl) were incubated for 10 min at room temperature with Greiss reagent (1% sulfanilamide, 0.1% N-[1-naphthyl]ethylenediamine, 5% H3PO4). The absorbance at 540 nm was measured using a microplate reader (Bio-Tek). Nitrite concentrations were determined by comparing the absorbance values for the test samples to a standard curve generated by serial dilution of 0.25 mM sodium nitrite.

**PKC stimulation.** Bone marrow cell suspensions were harvested as previously described and plated in 6-well plates ($3 \times 10^6$ cells/ml) with RPMI supplemented with 2 mM L-glutamine, 100 µg/ml streptomycin, 100 IU/ml penicillin, 1 mM sodium pyruvate, and 10% FBS for 18 h in the presence or not of PDBu (10 ng/ml). MDSCs were then isolated as previously described and prepared for Western blot analyses as described below.

**Western blotting.** MDSCs were isolated as previously described and immediately lysed with RIPA buffer in the presence of protease and phosphatase inhibitors. An equal amount of total protein lysates were subjected to 8% SDS-PAGE gel and transferred to PVDF membranes. Membranes were blocked in 5% BSA in PBS/Tween-20 for 1 h, and then probed with appropriate specific primary antibodies overnight at 4°C. Membranes were washed and incubated for 2 h at room temperature with secondary antibody-conjugated with peroxidase. Results were visualized by chemiluminescence detection using a SuperSignal West Dura Extended Duration Substrate (Thermo Fisher Scientific). Antibodies against p-PLCγ2 (Tyr1217), total β-catenin, p-PKC (pan; βII Ser660), and p-GSK3β (Ser9) were obtained from Cell Signaling Technology. Equal loading was assessed using anti–β-actin antibody (Sigma-Aldrich). Semi-quantifications of protein were determined using GeneTools software (Syngene).

**Statistical analysis.** Experiments were done in triplicate and analyzed using Student's *t* test. In calculating two-tailed significance levels for equality of means, equal variances were assumed for the two populations. Results were considered significant at $P < 0.05$.

We gratefully thank Tonia Thompson for research administration and Train Lupu for his help for the in vivo experiments (Department of Orthopaedics, Washington University). We thank Drs. Marina Cella and Marco Colonna for their gift of OT-1 mice. We thank the Washington University Bright Institute and Molecular Imaging Center (P50 CA94056ADD).

This work was supported by a National Institutes of Health (NIH) grant to R. Faccio (RO1 AR52921), Shriners Hospital Fund to R. Faccio, Bright Institute Pilot Research grant to R. Faccio, NIH grant to D.V. Novack (AR052705 and EB007568), and the Barnes-Jewish Foundation (D.V. Novack). This work was also supported by Barnes Jewish Hospital Cancer Frontier Fund (D.C. Linehan).

The authors declare no conflict of interest.

A.H. Capietto, S. Kim, and R. Faccio designed research; A.H. Capietto and S.K. performed research; D.E. Sanford, and D.C. Linehan provided patient samples; M. Hikida and T. Kumosaki provided PLCγ2cKO mice; A.H. Capietto, S. Kim, D.V. Novack, and R. Faccio analyzed and discussed the data; A.H. Capietto and R. Faccio wrote the paper.

**Submitted: 7 February 2013**
**Accepted: 6 September 2013**

## REFERENCES

Almand, B., J.I. Clark, E. Nikitina, J. van Beynen, N.R. English, S.C. Knight, D.P. Carbone, and D.I. Gabrilovich. 2001. Increased production of immature myeloid cells in cancer patients: a mechanism of immunosuppression in cancer. *J. Immunol.* 166:678–689.

Arguello, F., R.B. Baggs, and C.N. Frantz. 1988. A murine model of experimental metastasis to bone and bone marrow. *Cancer Res.* 48:6876–6881.

Barreda, D.R., P.C. Hanington, and M. Belosevic. 2004. Regulation of myeloid development and function by colony stimulating factors. *Dev. Comp. Immunol.* 28:509–554.

Batliner, J., E. Buehrer, E.A. Federzoni, M. Jenal, A. Tobler, B.E. Torbett, M.F. Fey, and M.P. Tschan. 2012. Transcriptional regulation of MIR29B by PU.1 (SPI1) and MYC during neutrophil differentiation of acute promyelocytic leukaemia cells. *Br. J. Haematol.* 157:270–274. http://dx.doi.org/10.1111/j.1365-2141.2011.08964.x

Brault, V., R. Moore, S. Kutsch, M. Ishibashi, D.H. Rowitch, A.P. McMahon, L. Sommer, O. Boussadia, and R. Kemler. 2001. Inactivation of the beta-catenin gene by Wnt1-Cre-mediated deletion results in dramatic brain malformation and failure of craniofacial development. *Development.* 128:1253–1264.

Bronte, V., E. Apolloni, A. Cabrelle, R. Ronca, P. Serafini, P. Zamboni, N.P. Restifo, and P. Zanovello. 2000. Identification of a CD11b(+)/Gr-1(+)/CD31(+) myeloid progenitor capable of activating or suppressing CD8(+) T cells. *Blood.* 96:3838–3846.

Castagna, M., Y. Takai, K. Kaibuchi, K. Sano, U. Kikkawa, and Y. Nishizuka. 1982. Direct activation of calcium-activated, phospholipid-dependent protein kinase by tumor-promoting phorbol esters. *J. Biol. Chem.* 257: 7847–7851.

Chalmin, F., S. Ladoire, G. Mignot, J. Vincent, M. Bruchard, J.P. Remy-Martin, W. Boireau, A. Rouleau, B. Simon, D. Lanneau, et al. 2010. Membrane-associated Hsp72 from tumor-derived exosomes mediates STAT3-dependent immunosuppressive function of mouse and human myeloid-derived suppressor cells. *J. Clin. Invest.* 120:457–471.

Clausen, B.E., C. Burkhardt, W. Reith, R. Renkawitz, and I. Forster. 1999. Conditional gene targeting in macrophages and granulocytes using LysMcre mice. *Transgenic Res.* 8:265–277

Dolcetti, L., E. Peranzoni, S. Ugel, I. Marigo, A. Fernandez Gomez, C. Mesa, M. Geilich, G. Winkels, E. Traggiai, A. Casati, et al. 2010. Hierarchy of immunosuppressive strength among myeloid-derived suppressor cell subsets is determined by GM-CSF. *Eur. J. Immunol.* 40:22–35. http://dx.doi.org/10.1002/eji.200939903

Feng, L., I. Reynisdóttir, and J. Reynisson. 2012. The effect of PLC-γ2 inhibitors on the growth of human tumour cells. *Eur. J. Med. Chem.* 54:463–469. http://dx.doi.org/10.1016/j.ejmech.2012.05.029

Filipazzi, P., V. Huber, and L. Rivoltini. 2012. Phenotype, function and clinical implications of myeloid-derived suppressor cells in cancer patients. *Cancer Immunol. Immunother.* 61:255–263

Gabitass, R.F., N.E. Annels, D.D. Stocken, H.A. Pandha, and G.W. Middleton. 2011. Elevated myeloid-derived suppressor cells in pancreatic, esophageal and gastric cancer are an independent prognostic factor and are associated with significant elevation of the Th2 cytokine interleukin-13. *Cancer Immunol. Immunother.* 60:1419–1430. http://dx.doi.org/10.1007/s00262-011-1028-0

Gabrilovich, D.I., and S. Nagaraj. 2009. Myeloid-derived suppressor cells as regulators of the immune system. *Nat. Rev. Immunol.* 9:162–174.

Gabrilovich, D.I., M.P. Velders, E.M. Sotomayor, and W.M. Kast. 2001. Mechanism of immune dysfunction in cancer mediated by immature Gr-1+ myeloid cells. *J. Immunol.* 166:5398–5406.

Gallina, G., L. Dolcetti, P. Serafini, C. De Santo, I. Marigo, M.P. Colombo, G. Basso, F. Brombacher, I. Borrello, P. Zanovello, et al. 2006. Tumors induce

a subset of inflammatory monocytes with immunosuppressive activity on CD8+ T cells. *J. Clin. Invest.* 116:2777–2790. http://dx.doi.org/10.1172/JCI28828

Greten, T.F., M.P. Manns, and F. Korangy. 2011. Myeloid derived suppressor cells in human diseases. *Int. Immunopharmacol.* 11:802–807.

Harada, N., Y. Tamai, T. Ishikawa, B. Sauer, K. Takaku, M. Oshima, and M.M. Taketo. 1999. Intestinal polyposis in mice with a dominant stable mutation of the beta-catenin gene. *EMBO J.* 18:5931–5942

Hamdorf, M., A. Berger, S. Schüle, J. Reinhardt, and E. Flory. 2011. PKCδ-induced PU.1 phosphorylation promotes hematopoietic stem cell differentiation to dendritic cells. *Stem Cells.* 29:297–306. http://dx.doi.org/10.1002/stem.564

Hashimoto, A., K. Takeda, M. Inaba, M. Sekimata, T. Kaisho, S. Ikehara, Y. Homma, S. Akira, and T. Kurosaki. 2000. Cutting edge: essential role of phospholipase C-gamma 2 in B cell development and function. *J. Immunol.* 165:1738–1742.

Kang, Y., P.M. Siegel, W. Shu, M. Drobnjak, S.M. Kakonen, C. Cordón-Cardo, T.A. Guise, and J. Massagué. 2003. A multigenic program mediating breast cancer metastasis to bone. *Cancer Cell.* 3:537–549. http://dx.doi.org/10.1016/S1535-6108(03)00132-6

Kirstetter, P., K. Anderson, B.T. Porse, S.E. Jacobsen, and C. Nerlov. 2006. Activation of the canonical Wnt pathway leads to loss of hematopoietic stem cell repopulation and multilineage differentiation block. *Nat. Immunol.* 7:1048–1056. http://dx.doi.org/10.1038/ni1381

Kortylewski, M., M. Kujawski, T. Wang, S. Wei, S. Zhang, S. Pilon-Thomas, G. Niu, H. Kay, J. Mulé, W.G. Kerr, et al. 2005. Inhibiting Stat3 signaling in the hematopoietic system elicits multicomponent antitumor immunity. *Nat. Med.* 11:1314–1321. http://dx.doi.org/10.1038/nm1325

Kusmartsev, S., and D.I. Gabrilovich. 2003. Inhibition of myeloid cell differentiation in cancer: the role of reactive oxygen species. *J. Leukoc. Biol.* 74:186–196. http://dx.doi.org/10.1189/jlb.0103010

Kusmartsev, S., and D.I. Gabrilovich. 2006. Effect of tumor-derived cytokines and growth factors on differentiation and immune suppressive features of myeloid cells in cancer. *Cancer Metastasis Rev.* 25:323–331. http://dx.doi.org/10.1007/s10555-006-9002-6

Kusmartsev, S., Y. Nefedova, D. Yoder, and D.I. Gabrilovich. 2004. Antigen-specific inhibition of CD8+ T cell response by immature myeloid cells in cancer is mediated by reactive oxygen species. *J. Immunol.* 172:989–999.

Kusmartsev, S., S. Nagaraj, and D.I. Gabrilovich. 2005. Tumor-associated CD8+ T cell tolerance induced by bone marrow-derived immature myeloid cells. *J. Immunol.* 175:4583–4592.

Lechner, M.G., C. Megiel, S.M. Russell, B. Bingham, N. Arger, T. Woo, and A.L. Epstein. 2011. Functional characterization of human Cd33+ and Cd11b+ myeloid-derived suppressor cell subsets induced from peripheral blood mononuclear cells co-cultured with a diverse set of human tumor cell lines. *J. Transl. Med.* 9:90. http://dx.doi.org/10.1186/1479-5876-9-90

Li, G., G. Wu, G. Zhao, G. Shi, G. Li, G. Zhang, G. Yin, G. Shuai, G. Wang, and G. Tao. 2013. HMGB1 recruits myeloid derived suppressor cells to promote peritoneal dissemination of colon cancer after resection. *Biochem. Biophys. Res. Commun.* In press.

Liu, Y., J.A. Van Ginderachter, L. Brys, P. De Baetselier, G. Raes, and A.B. Geldhof. 2003. Nitric oxide-independent CTL suppression during tumor progression: association with arginase-producing (M2) myeloid cells. *J. Immunol.* 170:5064–5074.

Lovatt, M., and M.J. Bijlmakers. 2010. Stabilisation of beta-catenin downstream of T cell receptor signalling. *PLoS ONE.* 5.

Ma, G., P.Y. Pan, S. Eisenstein, C.M. Divino, C.A. Lowell, T. Takai, and S.H. Chen. 2011. Paired immunoglobin-like receptor-B regulates the suppressive function and fate of myeloid-derived suppressor cells. *Immunity.* 34:385–395.

Marigo, I., E. Bosio, S. Solito, C. Mesa, A. Fernandez, L. Dolcetti, S. Ugel, N. Sonda, S. Bicciato, E. Falisi, et al. 2010. Tumor-induced tolerance and immune suppression depend on the C/EBPbeta transcription factor. *Immunity.* 32:790–802. http://dx.doi.org/10.1016/j.immuni.2010.05.010

Mazzoni, A., V. Bronte, A. Visintin, J.H. Spitzer, E. Apolloni, P. Serafini, P. Zanovello, and D.M. Segal. 2002. Myeloid suppressor lines inhibit T cell responses by an NO-dependent mechanism. *J. Immunol.* 168:689–695.

Movahedi, K., M. Guilliams, J. Van den Bossche, R. Van den Bergh, C. Gysemans, A. Beschin, P. De Baetselier, and J.A. Van Ginderachter. 2008. Identification of discrete tumor-induced myeloid-derived suppressor cell subpopulations with distinct T cell-suppressive activity. *Blood.* 111:4233–4244. http://dx.doi.org/10.1182/blood-2007-07-099226

Otero, K., I.R. Turnbull, P.L. Poliani, W. Vermi, E. Cerutti, T. Aoshi, I. Tassi, T. Takai, S.L. Stanley, M. Miller, et al. 2009. Macrophage colony-stimulating factor induces the proliferation and survival of macrophages via a pathway involving DAP12 and beta-catenin. *Nat. Immunol.* 10:734–743. http://dx.doi.org/10.1038/ni.1744

Pan, P.Y., G.X. Wang, B. Yin, J. Ozao, T. Ku, C.M. Divino, and S.H. Chen. 2008. Reversion of immune tolerance in advanced malignancy: modulation of myeloid-derived suppressor cell development by blockade of stem-cell factor function. *Blood.* 111:219–228. http://dx.doi.org/10.1182/blood-2007-04-086835

Pham, T.H., C. Benner, M. Lichtinger, L. Schwarzfischer, Y. Hu, R. Andreesen, W. Chen, and M. Rehli. 2012. Dynamic epigenetic enhancer signatures reveal key transcription factors associated with monocytic differentiation states. *Blood.* 119:e161–e171. http://dx.doi.org/10.1182/blood-2012-01-402453

Porembka, M.R., J.B. Mitchem, B.A. Belt, C.S. Hsieh, H.M. Lee, J. Herndon, W.E. Gillanders, D.C. Linehan, and P. Goedegebuure. 2012. Pancreatic adenocarcinoma induces bone marrow mobilization of myeloid-derived suppressor cells which promote primary tumor growth. *Cancer Immunol. Immunother.* 61:1373–1385. http://dx.doi.org/10.1007/s00262-011-1178-0

Roland, C.L., K.D. Lynn, J.E. Toombs, S.P. Dineen, D.G. Udugamasooriya, and R.A. Brekken. 2009. Cytokine levels correlate with immune cell infiltration after anti-VEGF therapy in preclinical mouse models of breast cancer. *PLoS ONE.* 4:e7669. http://dx.doi.org/10.1371/journal.pone.0007669

Sawant, A., J. Deshane, J. Jules, C.M. Lee, B.A. Harris, X. Feng, and S. Ponnazhagan. 2013. Myeloid-derived suppressor cells function as novel osteoclast progenitors enhancing bone loss in breast cancer. *Cancer Res.* 73:672–682. http://dx.doi.org/10.1158/0008-5472.CAN-12-2202

Scheller, M., J. Foerster, C.M. Heyworth, J.F. Waring, J. Löhler, G.L. Gilmore, R.K. Shadduck, T.M. Dexter, and I. Horak. 1999. Altered development and cytokine responses of myeloid progenitors in the absence of transcription factor, interferon consensus sequence binding protein. *Blood.* 94:3764–3771.

Scheller, M., J. Huelsken, F. Rosenbauer, M.M. Taketo, W. Birchmeier, D.G. Tenen, and A. Leutz. 2006. Hematopoietic stem cell and multilineage defects generated by constitutive beta-catenin activation. *Nat. Immunol.* 7:1037–1047. http://dx.doi.org/10.1038/ni1387

Schroeder, T., H. Kohlhof, N. Rieber, and U. Just. 2003. Notch signaling induces multilineage myeloid differentiation and up-regulates PU.1 expression. *J. Immunol.* 170:5538–5548.

Serafini, P., I. Borrello, and V. Bronte. 2006. Myeloid suppressor cells in cancer: recruitment, phenotype, properties, and mechanisms of immune suppression. *Semin. Cancer Biol.* 16:53–65.

Smith, M.R., D.W. Court, H.K. Kim, J.B. Park, S.G. Rhee, J.S. Rhim, and H.F. Kung. 1998. Overexpression of phosphoinositide-specific phospholipase Cgamma in NIH 3T3 cells promotes transformation and tumorigenicity. *Carcinogenesis.* 19:177–185. http://dx.doi.org/10.1093/carcin/19.1.177

Solito, S., E. Falisi, C.M. Diaz-Montero, A. Doni, L. Pinton, A. Rosato, S. Francescato, G. Basso, P. Zanovello, G. Onicescu, et al. 2011. A human promyelocytic-like population is responsible for the immune suppression mediated by myeloid-derived suppressor cells. *Blood.* 118:2254–2265. http://dx.doi.org/10.1182/blood-2010-12-325753

Tamura, T., T. Nagamura-Inoue, Z. Shmeltzer, T. Kuwata, and K. Ozato. 2000. ICSBP directs bipotential myeloid progenitor cells to differentiate into mature macrophages. *Immunity.* 13:155–165. http://dx.doi.org/10.1016/S1074-7613(00)00016-9

Wang, D., J. Feng, R. Wen, J.C. Marine, M.Y. Sangster, E. Parganas, A. Hoffmeyer, C.W. Jackson, J.L. Cleveland, P.J. Murray, and J.N. Ihle. 2000. Phospholipase Cgamma2 is essential in the functions of B cell and several Fc receptors. *Immunity.* 13:25–35. http://dx.doi.org/10.1016/S1074-7613(00)00005-4

Xiang, X., A. Poliakov, C. Liu, Y. Liu, Z.B. Deng, J. Wang, Z. Cheng, S.V. Shah, G.J. Wang, L. Zhang, et al. 2009. Induction of myeloid-derived suppressor

cells by tumor exosomes. *Int. J. Cancer.* 124:2621–2633. http://dx.doi.org/10.1002/ijc.24249

Youn, J.I., S. Nagaraj, M. Collazo, and D.I. Gabrilovich. 2008. Subsets of myeloid-derived suppressor cells in tumor-bearing mice. *J. Immunol.* 181:5791–5802.

Young, M.R., M.E. Young, and K. Kim. 1988. Regulation of tumor-induced myelopoiesis and the associated immune suppressor cells in mice bearing metastatic Lewis lung carcinoma by prostaglandin E2. *Cancer Res.* 48:6826–6831.

Younos, I., M. Donkor, T. Hoke, A. Dafferner, H. Samson, S. Westphal, and J. Talmadge. 2011. Tumor- and organ-dependent infiltration by myeloid-derived suppressor cells. *Int. Immunopharmacol.* 11:816–826. http://dx.doi.org/10.1016/j.intimp.2011.02.021

Yu, J., W. Du, F. Yan, Y. Wang, H. Li, S. Cao, W. Yu, C. Shen, J. Liu, and X. Ren. 2013. Myeloid-derived suppressor cells suppress antitumor immune responses through IDO expression and correlate with lymph node metastasis in patients with breast cancer. *J. Immunol.* 190:3783–3797. http://dx.doi.org/10.4049/jimmunol.1201449

Zea, A.H., P.C. Rodriguez, M.B. Atkins, C. Hernandez, S. Signoretti, J. Zabaleta, D. McDermott, D. Quiceno, A. Youmans, A. O'Neill, et al. 2005. Arginase-producing myeloid suppressor cells in renal cell carcinoma patients: a mechanism of tumor evasion. *Cancer Res.* 65:3044–3048.

Zhang, K., S. Kim, V. Cremasco, A.C. Hirbe, L. Collins, D. Piwnica-Worms, D.V. Novack, K. Weilbaecher, and R. Faccio. 2011. CD8+ T cells regulate bone tumor burden independent of osteoclast resorption. *Cancer Res.* 71:4799–4808. http://dx.doi.org/10.1158/0008-5472.CAN-10-3922